Plant Mol Biol Rep (2015) 33:1349–1360
DOI 10.1007/s11105-014-0817-y

ORIGINAL PAPER

Proteins Associated with Oxidative Burst and Cell Wall Strengthening Accumulate During Citrus-*Xanthomonas* Non-Host Interaction

T. Swaroopa Rani · Daisuke Takahashi · Matsuo Uemura · Appa Rao Podile

Published online: 21 November 2014

Abstract Citrus proteome changes at 8 and 48 h post inoculation (hpi) were analysed by both 2D gel electrophoresis and nano-LC-MS/MS proteomic approaches during interaction with *Xanthomonas axonopodis* pv. *citri* (*Xac*) and *Xanthomonas oryzae* pv. *oryzae* (*Xoo*) as host and non-host pathogens, respectively. A total of 256 proteins, 72 at 8 hpi and 184 at 48 hpi, differentially accumulated during citrus-*Xanthomonas* interaction. Of these, 67 and 115 proteins were specific to *Xac* and *Xoo* interaction, respectively. In addition, 64 proteins, 10 at 8 hpi and 54 at 48 hpi, variedly accumulated during both the interactions. Proteins related to photosynthesis, carbohydrate metabolism and protein synthesis were in low abundance during both the interactions resulting in reduced rate of photosynthesis. Proteins related to defence response, cell wall (CW) strengthening, lignin deposition and generation of reactive oxygen species (ROS) were in high abundance only during *Xoo* interaction. Whereas, during *Xac* interaction, proteins involved in antioxidant metabolism and CW loosening and/or elongation were in high abundance. The precise increase in abundance of these proteins during non-host interaction suggested an important role for CW fortification and ROS accumulation in non-host resistance in plants.

Keywords Proteome analysis · Citrus · *Xanthomonas* · nano-LC-MS/MS · 2DE · Pathogens

Abbreviations

NHR	Non-host resistance
LC-MS/MS	Liquid chromatography-tandem mass spectrometry
2DE	2D electrophoresis
Xac	*Xanthomonas axonopodis* pv. *citri*
Xac	*Xanthomonas oryzae* pv. *oryzae*
ROS	Reactive oxygen species
PRX	Peroxidase
SOD	Superoxide dismutase
APX	Ascorbate peroxidase
XTH	Xyloglucan endotransglycosylase/hydrolase
CW	Cell wall

Introduction

Plant-microbe interactions depend on the combination of interacting partners, developmental stage of plant and environmental signals. Plants are resistant to a majority of pathogens they encounter and are susceptible to a limited number of specifically adapted pathogens. The ability of plants to combat many pathogens is due to a form of immunity called non-host resistance (NHR), in which an entire plant species is resistant to all isolates of a pathogen that are able to infect other plant species (Senthil-Kumar and Mysore 2013). NHR is a multi-layered defence response, involving interplay of both constitutive barriers and inducible reactions activated after recognition of pathogen-associated molecular patterns (PAMPs) at the plant cell surface including the extracellular matrix (ECM) (Nurnberger and Lipka 2005; Schulze-Lefert and Panstruga 2011; Uma et al. 2011).

Electronic supplementary material The online version of this article (doi:10.1007/s11105-014-0817-y) contains supplementary material, which is available to authorized users.

T. S. Rani · A. R. Podile (✉)
Department of Plant Sciences, School of Life Sciences, University of Hyderabad, Hyderabad 500 046, Telangana, India
e-mail: arpsl@uohyd.ernet.in

A. R. Podile
e-mail: podilerao@gmail.com

D. Takahashi · M. Uemura
Cryobiofrontier Research Center and United Graduate School of Agricultural Sciences, Iwate University, Morioka 020-8550, Japan

NHR is a quantitative trait controlled by multiple genes. Therefore, silencing or mutating gene(s) that possibly have a role in NHR may result only in partial compromise of NHR. Efficient signal perception and robustness of individual pathogen recognition events are characteristics of NHR (Nurnberger and Scheel 2001). During pathogen invasion, plants perceive the PAMPs and activate several inducible downstream defence pathways. Such induced defence responses restrict non-host pathogen growth with or without occurrence of hypersensitive reaction (HR)-associated cell death (Oh et al. 2006). However, adapted pathogens can suppress such induced plant defence responses by effector proteins. The effector molecules of non-host pathogens are recognized to activate a more robust form of plant immunity (Schulze-Lefert and Panstruga 2011) that is not well understood. We, therefore, need to understand more details of this form of immunity known as NHR in plants.

Most of the genes that contribute to bacterial NHR are indispensable for the plant because they are required for basic plant metabolism, signalling pathways and defence response (Senthil-Kumar and Mysore 2013). Daurelio et al. (2011, 2013) identified a set of transcription factors and gene transcripts closely associated with NHR against non-host bacterial pathogens. Comparative gene expression profiling of *Arabidopsis* during compatible and non-host bacterial interactions revealed both common and distinct expression of several genes (Tao et al. 2003), indicating that plant defence responses are dependent on the speed and magnitude of the expression of defence genes. The events occurring in non-host interaction were dissected using mutant screening, forward genetics and microarray analysis (Kang et al. 2003; An and Mou 2012; Li et al. 2012a; Daurelio et al. 2011, 2013). However, limited details are available about the proteins involved in NHR, particularly in perennial species.

Proteomics has been a useful technique to gain in-depth understanding of many aspects of the plant–pathogen interactions (Zimaro et al. 2011). A combination of gel-based and gel-free methods proved complementary (Nouri and Komatsu 2010) in analysing the proteome. A label-free liquid chromatography-tandem mass spectrometry (LC-MS/MS) allows quantitative comparison of the proteomes under different conditions (Li et al. 2012b; Takahashi et al. 2012, 2013). Analysis of the citrus ECM-associated secretome changes during host and non-host *Xanthomonas* interaction in our earlier study suggested an active involvement of classical and non-classical secretory proteins of ECM in execution of NHR (Rani and Podile 2014). Here, we analysed global citrus leaf proteome changes during interaction with *Xanthomonas axonopodis* pv. *citri* (*Xac*) and *Xanthomonas oryzae* pv. *oryzae* (*Xoo*) as host and non-host pathogens, respectively, through 2D electrophoresis (2DE) and high-throughput LC-MS/MS approaches. We report specific and differentially accumulated proteins associated with reactive oxygen species (ROS) metabolism and cell wall strengthening that are involved in NHR. We also identified a set of overlapping proteins that are common in both compatible and non-host interactions of citrus with Xanthomonads.

Materials and Methods

Plant Material and Pathogen Inoculation

Sweet orange [*Citrus sinensis* (L.) Osbeck] grafted on Rangpur lime (*Citrus limonia* Osb.) plants obtained from Shiridi Sai Baba Nursery, Sangareddy, Telangana, India were pressure-infiltrated into the abaxial side of the leaves on both sides of the midrib using a 1 mL tuberculin syringe as described by Rani and Podile (2014). Leaves inoculated with *Xac*, *Xoo* and 10 mM $MgCl_2$ were harvested at different hours post inoculation (hpi) and frozen in liquid nitrogen immediately.

Sampling of Citrus Leaf Protein Profiles in Response to Xanthomonads

In citrus-*Xoo* interaction, visible defence response occurred at 16 hpi whereas, in *Xac* challenge, disease symptoms appeared at 48 hpi (Rani and Podile 2014). Therefore, for citrus leaf proteome analysis, 8 hpi, where no visible defence response observed and 48 hpi of *Xanthomonas* challenge were selected as early and late time points of interaction, respectively. Proteome changes were analysed to study the defence responses in citrus leaves during interaction with *Xac* (host) and *Xoo* (non-host) pathogens, by both gel-based 2DE and nano-LC-MS/MS proteomic approaches.

Isolation of Total Leaf Protein

Citrus leaves of mock, *Xac* and *Xoo* challenge, collected after 8 and 48 hpi, were immediately frozen in liquid nitrogen and stored at −80 °C until further use. Total leaf proteins were extracted as described by Isaacson et al. (2006) with minor modification. One gram of the frozen leaf tissue was ground to fine powder with liquid nitrogen, followed by re-suspension in the extraction buffer [0.5 M Tris–HCl (pH 7.5), 0.7 M sucrose, 0.1 M KCl, 50 mM EDTA, 2 % β mercaptoethanol and 1 mM PMSF] in a ratio 1:4 (*w*/*v*). The samples were mixed for 10 min at 4 °C and centrifuged at 12,000*g* for 20 min, at 4 °C. An equal volume of phenol saturated with Tris–HCl (pH 7.5) was added to the supernatant, mixed for 30 min at 4 °C and centrifuged at 5,000*g* for 30 min at 4 °C. The upper phenolic phase was collected. The same step was repeated. The proteins in the phenolic phase were precipitated with four volumes of 0.1 M ammonium acetate in methanol at −20 °C overnight and centrifuged at 10,000*g* at 4 °C for

30 min. The precipitate was washed thrice with ice-cold methanol and twice with ice-cold acetone and air dried for few minutes. The pellet was solubilised in rehydration solution [8 M (*w*/*v*) urea, 2 M (*w*/*v*) thiourea, 4 % (*w*/*v*) CHAPS, 30 mM dithiothreitol (DTT)]. Concentration of proteins was measured by amido black method with bovine serum albumin as standard (Henkel and Bieger 1994). All protein samples were stored at −80 °C prior to electrophoresis.

2D Electrophoresis and Data Analysis

Isoelectric focusing (IEF) of total leaf proteins in an Ettan IPGphor III electrophoresis unit (GE Healthcare) using 18 cm IPG strips (4–7 pH linear gradient; GE Healthcare) and data analysis were essentially same as described by Rani and Podile (2014). After first dimension separation of proteins, the strips were stored at −80 °C until 2D analysis. Protein spots on 2DE gels were visualized with colloidal coomassie staining (Wang et al. 2007), and the images were acquired in image scanner (GE Healthcare). The differentially accumulated proteins were analysed using Image Master 2D Platinum version 6 image analysis (GE Healthcare). Percent of coefficient of variance (%CV) of protein spots on the gels was calculated according to Asirvatham et al. (2002). The relative change in protein levels between the pathogen-challenged and mock-challenged gels was considered based on their ratio. The protein spots with a ratio of 1 between treated and mock were considered as no change and ±0.5 as increase or decrease in abundance. The differentially accumulated protein spots were selected for further analysis after the Student's *t* test ($P<0.05$, $n=6$).

Trypsin Digestion

Differentially accumulated protein spots were excised from the colloidal coomassie-stained gels. Gel pieces were washed with 50 % acetonitrile (ACN) in 25 mM ammonium bicarbonate (NH_4HCO_3) until the gel pieces were destained. Trypsin digestion was performed to the gel pieces according to Rani and Podile (2014). The trypsin-digested peptides were dissolved in 5 μL of 1:1 ACN and 1 % TFA. To 1 μL of this mixture, 1 μL of freshly prepared α-cyano-4-hydroxycinnamic acid (CHCA) matrix in 50 % ACN and 1 % TFA (1:1) were added. Finally, 1 μL was spotted on target plate.

Protein Identification

Matrix-assisted laser desorption/ionization time-of-flight mass spectrometry (MALDI-TOF MS) data analysis was conducted with a MALDI-TOF/TOF mass spectrometer, a Bruker AutoXex mass spectrometer (Bruker-Franzen, Bremen, Germany). Mass spectral data (MS/MS fragment ion) was searched in Swisspot, EST-other and NCBIInr databases using MASCOT program (http://www.matrixscience.com, Matrix Science Ltd., London, UK) employing Biotools software (Bruker Daltonics) for protein identification. The taxonomic category was set to *Viridiplantae* (green plants), and other search parameters were fixed modification of carbamidomethyl (C), variable modification of oxidation (M), enzyme trypsin, peptide tolerance of 100 ppm and MS/MS tolerance of 0.4 Da. The protein identity was accepted only if the MASCOT probability was at significant threshold level ($P<0.05$), and at least two peptides matched.

Nano-LC-MS/MS Analysis of Whole Cell Proteins

Sample Preparation and In-Gel Trypsin Digestion for Nano-LC-MS/MS Analysis

Approximately 5 μg protein within 10 μL was mixed with equal volume of SDS sample buffer (2 % [*w*/*v*] SDS, 50 mM Tris–HCl [pH 6.8], 6 % [*v*/*v*] β-mercaptoethanol, 10 % [*w*/*v*] glycerol and bromophenol blue) and heated at 95 °C for 20 min to dissolve proteins. Protein samples were separated on 7.5 % polyacrylamide pre-cast gels (PAGEL NPU-7.5L; ATTO Corporation, Tokyo, Japan) at 100 V until the upper end of sample dye band enters 2 mm from the well. Gel slices from the well to 2 mm in front of the dye were cut into four equal pieces and kept in 1.5 mL microtubes. In-gel tryptic digestion was performed for nano-LC-MS/MS according to Li et al. (2012a)). Trypsin-digested peptides were extracted according to Shevchenko et al. (1996). The peptide samples were desalted and purified with SPE C-TIP (AMR, Tokyo, Japan), and the volume was adjusted to 15 μL.

Mass Spectroscopy

Purified and trypsin-digested peptides were trapped and concentrated in a trap column (L-column Micro 0.3×5 mm; CERI, Japan) using an ADVANCE UHPLC system (MICHROM Bioresources, Auburn, CA). Subsequently, peptides were eluted with 0.1 % (*v*/*v*) formic acid in acetonitrile. Then, valve was switched to connect trap column with Magic C18 AQ nanocolumn (0.1×150 mm; MICHROM Bioresources). A linear gradient of acetonitrile (from 5 % [*v*/*v*] to 45 % [*v*/*v*]) at a flow rate of 500 nL/min for 100 min was used to separate peptides. Peptide ionization was performed at a spray voltage of 2.0 kV. LTQ Orbitrap XL mass spectrometer (Thermo Fisher Scientific, Waltham, MA) equipped with Xcalibur software (version 2.0.7, Thermo Fisher Scientific) was used for mass analysis. Full-scan mass spectra were obtained under the data-dependent scanning mode, in the range of 400 to 1,800 *m*/*z* with a resolution of 30,000. To the ten most intense ions, collision-induced fragmentation was

applied at a threshold above 500. These experiments were performed with four biological replicates.

Label-Free Protein Quantification and Protein Identification

Raw files of MS/MS spectra were obtained from nano-LC-MS/MS. Semi-quantitative analysis of differentially accumulated proteins, during pathogen challenge at 8 and 48 hpi, was performed with Progenesis LC-MS software (version 4.0, Nonlinear Dynamics, Newcastle, UK) as described by Takahashi et al. (2013). Briefly, raw files of MS/MS spectra were imported to Progenesis LC-MS software. LC-MS runs represented as *m/z* and retention time were aligned, and reference run was selected. Quantitative abundance ratio of each feature between the reference run and the runs being normalized was calculated, and normalization factor was derived from these ratios. Normalization was performed in Progenesis LC-MS software (as described in the following URL http://www.nonlinear.com/support/progenesis/lc-ms/faq/v4.1/how-normalisation-works.aspx). In this process, peptides that were compared between mock and pathogen challenge were tagged with ANOVA ($P<0.05$) and maximum fold change (>2.0). The resultant peptides were re-analyzed with the Mascot search engine (version 2.3.02, Matrix Science, London, UK) using exported mgf files from Progenesis software. Proteins were identified by searching against the NCBInr Green Plants database (version 20130531 comprising 25510175 sequences) with following parameters (one missed cleavage was allowed). Carbamidomethylation of cysteines and oxidation of methionine were set as fixed and variable modifications, respectively. Peptide mass tolerance was 5 ppm, and MS/MS tolerance was 0.6 Da. Peptide charges were set to +1, +2 and +3. To generate a representative list of proteins with increased reliability, the proteins were defined as "identified" if the protein matched at least one unique top-ranking peptide with an expected value ≤0.05. If a peptide was assigned to multiple proteins, the highest scoring protein was selected in the list. As peptides were filtered with criteria including mass tolerance (5 ppm), fragment ion mass tolerance (0.6 Da), ion score cut-off (<0.05) and unique/highest scoring according to confidence of the data, each peptide has a certain level of confidence. Therefore, proteins with single peptides of high confidence were also considered for quantification. Proteins responded to host and non-host pathogen, at 8 and 48 hpi, were functionally classified according to Bevan et al. (1998). Heat maps were generated for $\log_2$-transformed average fold change of the differentially accumulated proteins of *Xac* and *Xoo* challenge using PermutMatrix software (Caraux and Pinloche 2005; Meunier et al. 2007).

H_2O_2 Measurement, Staining and Lipid Peroxidation

H_2O_2 was measured according to Velikova et al. (2000). Briefly, 0.5 g of leaf tissue was homogenised in ice-cold 0.1 % trichloroacetic acid and centrifuged at 12,000*g* for 15 min at 4 °C. To 0.3 mL of supernatant, 1.7 mL potassium phosphate buffer (pH 7.0) and 1 mL of 1 M potassium iodide were added. After 5 min of incubation, oxidation product were measured at A_{390}. A standard curve prepared from known concentrations of H_2O_2 was used to quantify H_2O_2 as μmol g^{-1} fresh weight of leaf tissue. H_2O_2 was detected *in situ* by 3,3′-diaminobenzidine (DAB) staining (Thordal-Christensen et al. 1997) and viewed under light microscope. Lipid peroxidation was measured as malonic dialdehyde (MDA) content as described by Heath and Packer (1968).

ROS-Metabolizing Enzyme Assays

Leaf samples (0.5 g) were homogenised in 100 mM potassium phosphate buffer pH 7.0 containing 0.5 mM EDTA, 0.1 mM phenylmethylsulphonyl fluoride (PMSF) and 2 % polyvinylpyrrolidone in a pre-chilled pestle and mortar. The homogenate was centrifuged at 4 °C for 30 min at 15,000*g*. The supernatant was used for enzyme assays. Superoxide dismutase (SOD) activity was assayed by measuring the inhibition of photochemical reduction of nitroblue tetrazolium (NBT) at A_{560} (Beauchamp and Fridovich 1971). One unit of the SOD was defined as amount of enzyme required to inhibit reduction of NBT by 50 %. Peroxidase (POD) activity was measured as increase in absorbance at A_{470} due to oxidation of guaiacol to tetraguaiacol. The ascorbate peroxidase (APX) activity was determined measuring the decrease in absorbance at A_{290} due to reduction of ascorbate (Nakano and Asada 1987) and calculated using extinction coefficient 2.8 mM^{-1} cm^{-1} for reduced ascorbate and expressed as mM min^{-1} mg^{-1} protein.

Lignin Deposition

Leaves harvested at different time points after pathogen challenge were stained for lignin deposition by phloroglucinol-HCl method (Vallet et al. 1996). Mock- and pathogen-challenged leaves were incubated overnight in a solution of 1 % phloroglucinol in 100 % methanol. The leaf tissue was cleared by incubating in chloral hydrate and mounted on slides. A few drops of concentrated HCl was added, covered with a cover slip, and viewed immediately. After ~10 min, lignified structures appeared cherry red-orange that faded within 4 h.

Measurement of Photosynthesis

One centimetre leaf discs of mock/pathogen-inoculated regions of citrus leaves of 8 and 48 hpi was cut and blotted dry. Later, the discs were transferred into the oxygen electrode chamber (LD-2, Hansatech Instruments Ltd., King's Lynn, UK) and determined the rate of photosynthetic according to Talla et al. (2011).

Statistics

Results of the biochemical analysis were represented as mean ±standard deviations (n=6). The ANOVA and Tukey test were performed between mock and *Xac*/*Xoo* interaction and between *Xac* vs *Xoo* interaction using the statistical package, Sigma Plot 10.0. Three biological replicates with two technical replications were analysed in gel-based approach. The nano-LC-MS/MS-based analysis was performed in quadruples for mock, *Xac*- and *Xoo*-challenged samples of each time point (8 and 48 hpi), and proteome differences were determined using Student's t test.

Results

Citrus Leaf Protein Profiles in Response to Xanthomonads

Gel-Based 2DE Approach

A total of 480 protein spots were resolved on 2DE gels stained with coomassie brilliant blue dye in a pI range of 4–7. The molecular mass of the proteins ranged between 10 and 100 kDa. The coefficient of variance (CV) was 23 % indicating minimum gel to gel variation. Twenty-three protein spots that significantly and differentially accumulated during citrus-*Xanthomonas* interactions were identified through MALDI-TOF MS/MS analysis. The fold change of the differentially accumulated proteins in pathogen and mock challenge, accession number and source organism are shown in (Supplementary Table S1). The representative 2DE gels of proteins from the citrus leaves of mock/*Xac*/*Xoo* inoculation are shown in Fig. 1. Fifteen proteins were accumulated differentially in both the types of citrus-pathogen interaction. Among them, six proteins (spot no. 1, 7, 8, 20, 21 and 22) were up-accumulated and four proteins (spot no. 10, 13, 14 and 19) were down-accumulated during both host and non-host interactions. ATP synthase subunit α and γ were in high abundance during *Xac* interaction, and decreased during *Xoo* interaction, while it was reverse with 17.6 kDa heat shock protein (HSP). GDP-mannose 3′,5′-epimerase and NAD-dependent epimerase (spots 3 and 4, respectively) were up-accumulated only in citrus-*Xac* interaction. On the other hand, *Xoo* inoculation significantly up-accumulated S-adenosylmethionine synthase and HSP90 (spots 5 and 9, respectively). Chlorophyll a,b protein (spot 20 and 21) and phosphoribulokinase (spot 15 and 23) were identified in more than one spot.

Nano-LC-MS/MS-Based Approach

Nano-LC-MS/MS analysis lead to the identification of 495 and 553 proteins that were across the treatments for the early (i.e., 8 hpi) and late (i.e., 48 hpi) time points, respectively. A total of 137 and 280 proteins accumulated differentially at 8 and 48 hpi, respectively, during citrus-*Xanthomonas* interaction. The molecular mass of the identified proteins ranged from 2 to 406 kDa, with 65 % of these proteins ranging from 23 to 80 kDa. The pI value of the proteins ranged from 4 to 11. At 8 and 48 hpi, statistically significant change was not detected for about two thirds of the proteins. Twenty-one proteins were commonly identified in gel-based and non-gel-based proteome datasets (Fig. 2).

Functional Categorization of Differentially Accumulated Proteins

Proteins that significantly varied in their accumulation were classified in to 13 functional categories (Supplementary Tables S2–S5). A relatively large number of proteins (26 and 25 % of 8 and 48 hpi proteins, respectively) were not assigned to any function categorized as unknown, therefore, not included for further analysis. A marginal difference in percentage of 13 different functional categories was observed at both time points (Supplementary Fig. S1). Similar percentage of functional categories was observed at both the time points, with there being slightly less for disease/defence and slightly more for energy, metabolism and protein destination and storage at 48 hpi (Supplementary Fig. S1b). On separation of host and non-host responsive proteins, at 8 and 48 hpi, into the proteins of high and low abundance, majority of the differentially accumulated proteins were related to energy, metabolism, defence, cell structure, antioxidants, protein synthesis, and protein destination and storage (Fig. 3).

Differential Accumulation of Proteins at 8 and 48 hpi

During early stages of interaction of citrus (8 hpi) with *Xac* and *Xoo*, nine proteins were up-accumulated and an equal number of proteins were also down-accumulated during both host and non-host interactions (Supplementary Fig. S2a), at different amplitudes. Whereas, in *Xoo* and *Xac* interactions with citrus resulted in up-accumulation of 22 and 11 proteins, respectively (Supplementary Table S2). Similarly, 7 proteins in *Xoo* interaction and 14 proteins in *Xac* interaction were

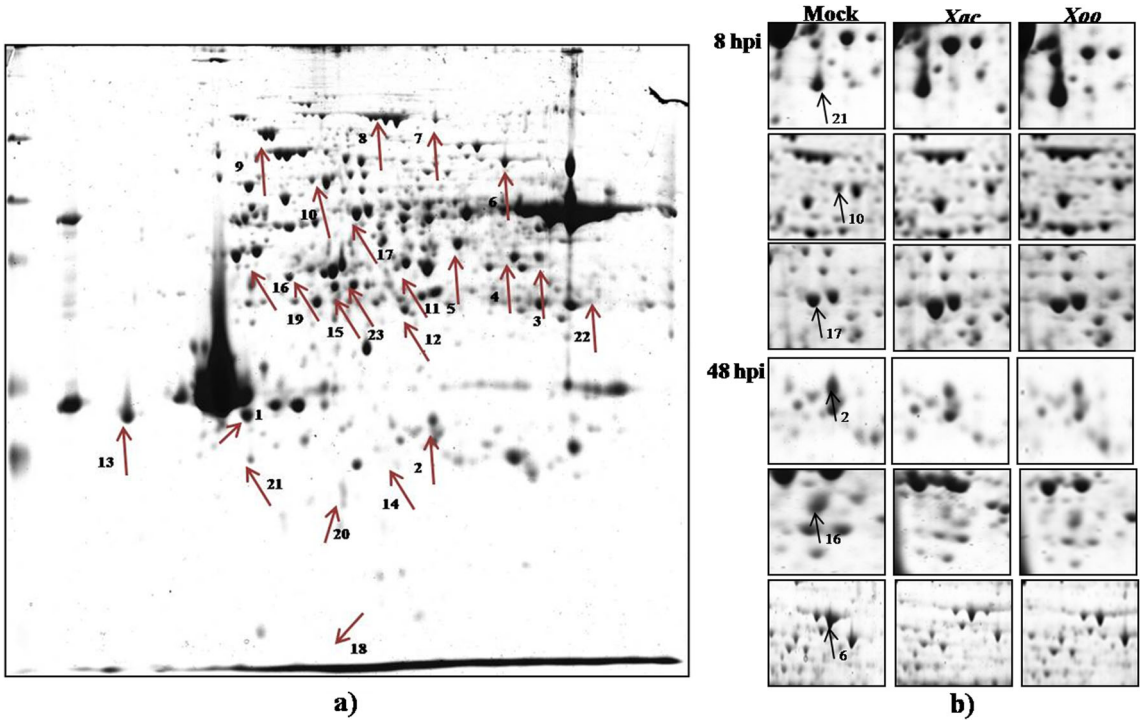

Fig. 1 2DE analysis of citrus leaf proteome in response to *Xac* and *Xoo* challenge: **a** Representative 2D gel image of citrus leaf proteome. 2DE was performed using an equal amount (600 μg) of leaf proteome on 18 cm immobiline dry strips with linear pH gradients from 4 to 7. Gels were stained with colloidal coomassie blue G-250. **b** Magnified views of some differentially expressed spots. *Arrows* and *numbers* represent the protein spots that altered significantly ($P<0.05$) and selected for MS/MS analyses

down-accumulated, respectively. In both host and non-host interactions, at 48 hpi, 31 were in high abundance and 25 proteins were in low abundance (Supplementary Fig. S2b). But, there was a high abundance of 40 and 30 proteins in *Xoo* and *Xac* interaction, respectively (Supplementary Table S3). Forty-six proteins in *Xoo* interaction and 14 proteins during *Xac* challenge were down-accumulated. Differential accumulation was mostly persistent to a single sampling time point, and 11 proteins were differentially accumulated at both 8 and 48 hpi (Supplementary Fig. S2c, Supplementary Table S5). The proportion of proteins overlapping between both pathogen interactions was next to the proteins responding only to *Xoo* (Supplementary Table S4).

Different proportions of up-accumulated and down-accumulated proteins in *Xac* and *Xoo* challenge were categorized in terms of specific functional groups. Compared to early hours of interaction, higher number of proteins overlapped at 48 hpi between *Xac* and *Xoo* interaction. In the plant-host and non-host pathogen interactions, proteins with significant fold change values responded specifically to either *Xac* or *Xoo*. Proteins commonly responded to both the pathogens were further analyzed, and heat map profiles were generated (Fig. 4). The proteins that varied their abundance after *Xac* and *Xoo* challenge were categorized as those responded to either *Xac* or *Xoo* as groups I and II, respectively, and those responded to both *Xac* and *Xoo* as group III. Heat map profiling indicated that proteins related to photosynthesis were predominant among the proteins co-accumulation during interaction with both the pathogens at 48 hpi.

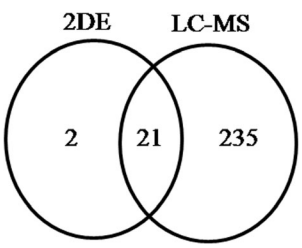

Fig. 2 Diagrammatic representation of proteins identified through gel-based and non-gel-based proteomics: Distribution of 2DE- and nano-LC-MS/MS-identified differentially regulated proteins during *Xanthomonas* interaction was displayed along with commonly identified proteins

Biochemical Changes in Citrus During Compatible and Non-Host Interactions

We have measured H_2O_2 levels and assayed ROS metabolism-related enzymes like POD, SOD and APX. H_2O_2 levels and lipid peroxidation increased in both types of interactions. But, the magnitude was high during non-host interaction (Fig. 5a, b). A 2.6-fold rise in H_2O_2 accumulation in citrus leaves occurred by 24 hpi, upon *Xoo* challenge, and 1.6-fold rise upon *Xac* challenge in comparison with mock inoculation at 48 hpi (Fig. 5a). Lipid peroxidation peaked by 2.2-fold at 24 hpi during *Xoo* interaction and marginally

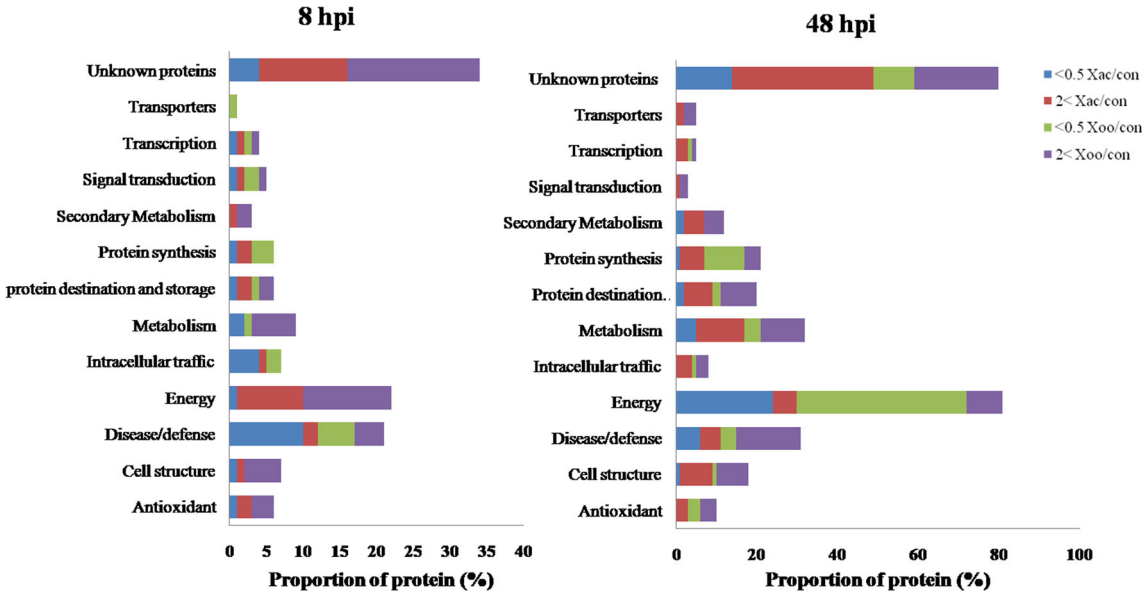

Fig. 3 Distribution of modulated proteins in response to *Xac* and *Xoo* interactions: Proportions in functional categories of citrus leaf proteins increased or decreased during *Xac* and *Xoo* challenge at 8 hpi (*right panel*) and at 48 hpi (*left panel*) were represented in bars with different colours

increased during *Xac* interaction at 24 and 48 hpi (Fig. 5b). Further, H_2O_2 accumulation was detectable at 24 hpi with 3,3′-diaminobenzidine (DAB) staining (Fig. 5c). However, in mock- and *Xac*-challenged leaves, H_2O_2 deposition was not detectable (Fig. 5c).

The SOD activity sharply increased by 4-fold compared to mock challenge during *Xoo* challenge, while it was only 1.8-fold higher in *Xac* interaction at 24 hpi (Fig. 6b). In contrast, APX activity was at its peak (5.5-fold) at 16 hpi during *Xac* interaction, whereas, a 2.5-fold increase was observed during *Xoo* challenge (Fig. 6c). POD activity was more during *Xoo* interaction from 16 to 48 hpi, in comparison with *Xac* and mock challenge. The increase in POD activity was 2.6-fold in *Xoo* challenge at 24 hpi, compared to *Xac* and mock challenge (Fig. 6a). Lignin deposition was visible as reddish brown spots in *Xoo*-challenged citrus leaves at 72 hpi, whereas, in *Xac*- and mock-challenged leaves, there was no lignin deposition (Fig. 7). Effect of pathogen challenge on photosynthetic oxygen evolution in citrus leaves was measured through oxygraph. Oxygen evolution decreased at 48 hpi in both the interactions. The decrease was 1.27-fold higher in *Xoo*-challenged leaves compared to *Xac*-challenged citrus leaves (Supplementary Fig. S3).

Discussion

We approached NHR of citrus with a comparative proteome analysis during host (*Xac*) and non-host (*Xoo*) pathogen interactions. Functional categorization of proteins revealed that a relatively large number of differentially accumulated proteins belonged to unknown category, compared to the other functional categories, possibly due to the unresolved status of the citrus genome. Proteins related to energy, metabolism, disease/defence, cell structure and antioxidant metabolism, which could decide the outcome of plant–pathogen interaction, were predominant in citrus-*Xanthomonas* interaction (Fig. 3).

Proteins accumulated in response to *Xoo* challenge were different from those accumulated in response to *Xac* in citrus. A relatively small number of proteins (23 and 22.6 % at 8 and 48 hpi, respectively) were in high abundance during *Xac* interaction than in *Xoo*-challenged citrus leaves (Fig. 4), consistent with the magnitude of the establishment of defence responses in these two interactions. There was a considerable similarity (13.5 and 23 % at 8 and 48 hpi, respectively) in protein profiles of citrus against host and non-host pathogens, that was considerably high at late hours of interaction.

Accumulation of ROS-Generating and Signal Transduction-Related Proteins during NHR

Among the proteins that commonly varied during interaction with Xanthomonads, signalling-related proteins like 14-3-3 protein, G-box-binding factor and leucine-rich repeat protein differentially accumulated at 8 hpi (Fig. 4, group III). On the other hand, acid phosphatase, Ras-related proteins and 14-3-3 proteins were specifically up-accumulated during *Xoo* interaction at 48 hpi (Fig. 4, group II). These proteins were known to be involved in signal transduction at multiple levels in response to biotic and abiotic stresses (Roberts et al. 2002). G-box-binding proteins were regarded as key molecular switches for the modulation of many plant-specific signalling

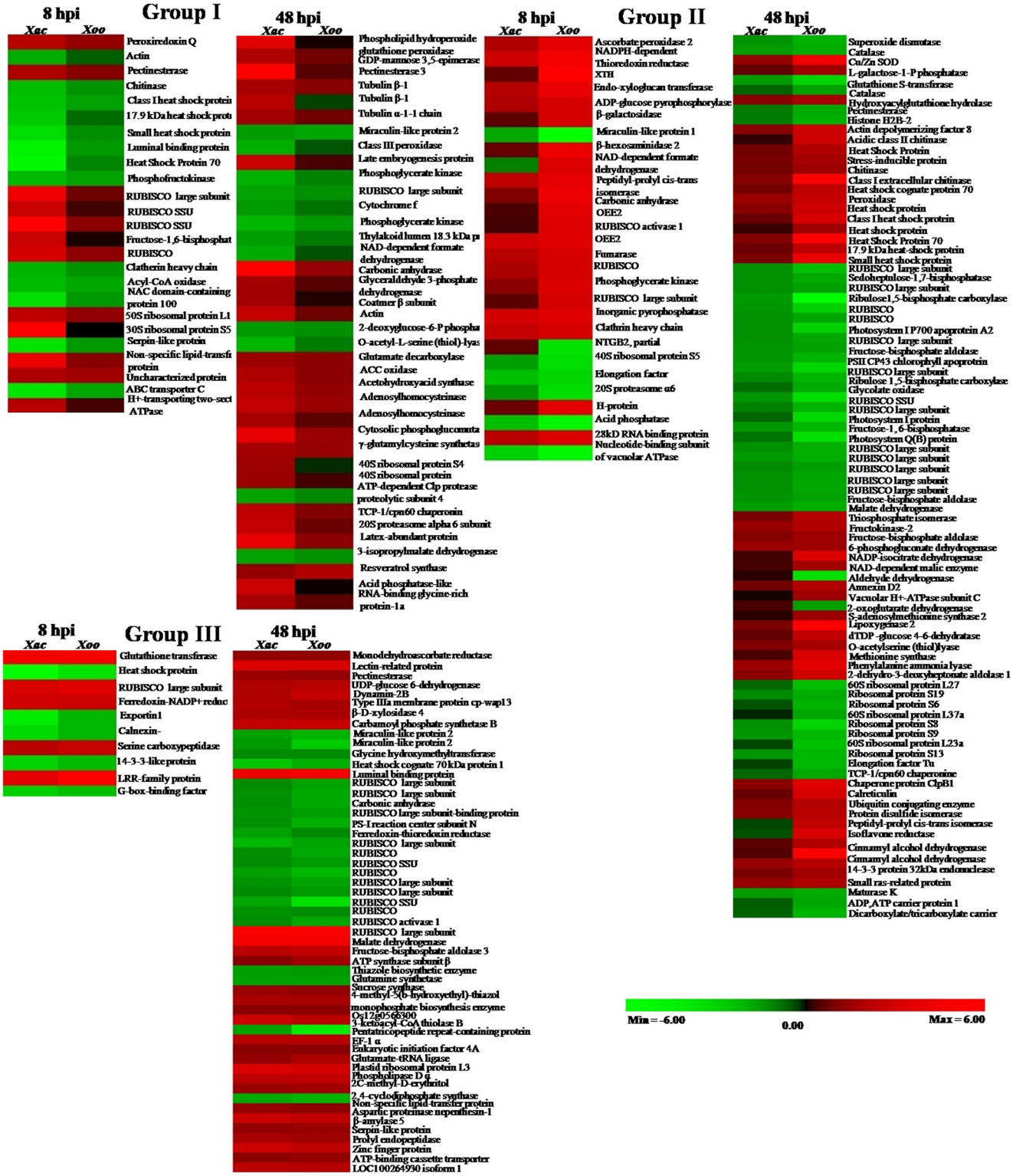

Fig. 4 Heat map profile of differentially regulated proteins during citrus-*Xanthomonas* interactions: Colours indicate the amount of protein accumulation in response to *Xac* or *Xoo* relative to Mock. Groups I and II consist of proteins that had specific regulation during *Xac* or *Xoo* challenge, respectively. Group III represents proteins that generally accumulated during both the interactions

pathways (Ma 2007). Differential accumulation of G-box protein was observed in compatible and incompatible white pine-blister rust interactions (Zamany et al. 2012). The co-accumulation of these signalling proteins during both *Xac* and *Xoo* interaction could be a part of PAMP-triggered basal defence system.

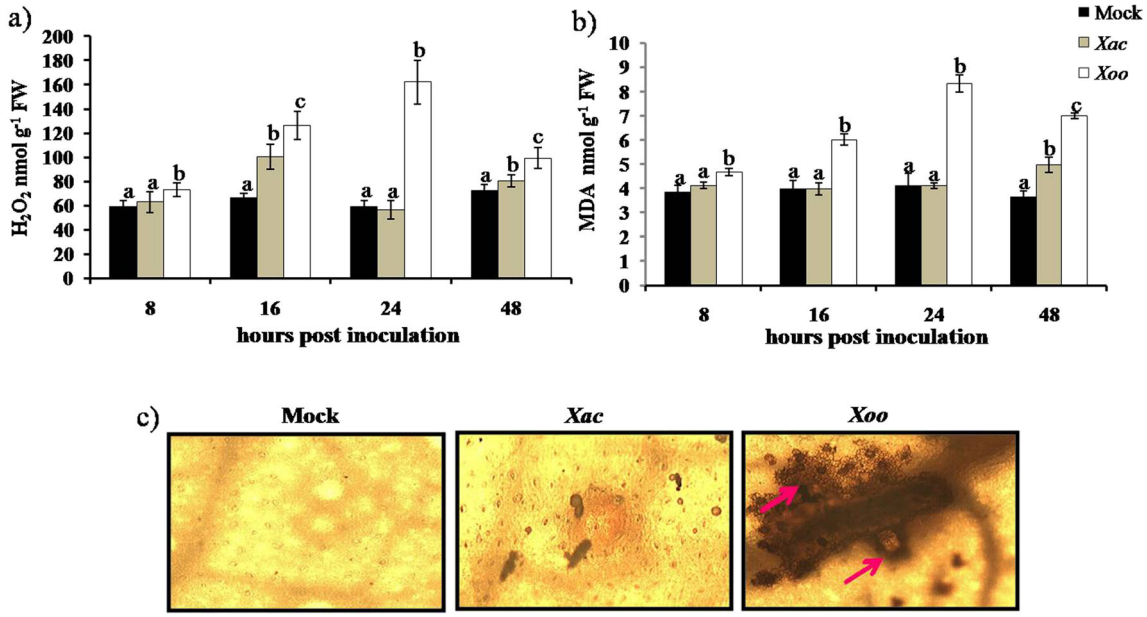

Fig. 5 Measurement of H_2O_2 levels and lipid peroxidation during citrus-Xanthomonas interaction: **a** H_2O_2 accumulation and **b** lipid peroxidation levels were measured during time course of interaction of citrus with *Xac* and *Xoo* and **c** ROS accumulation was determined by DAB staining at 24 hpi (indicated by *arrows*). *Error bars* indicate standard deviation of the mean from three independent experiments. The ANOVA and Tukey test were performed between mock and *Xac*/*Xoo* interaction and between *Xac* vs *Xoo* interaction. *Bars followed by same alphabets* are not significantly different at $P \leq 0.05$

Oxidative burst was an early event associated with the defence response leading to generation of ROS in plant cell (Overmyer et al. 2003). In this study, free radical scavenger like glutathione S-transferase (GST) was in high abundance

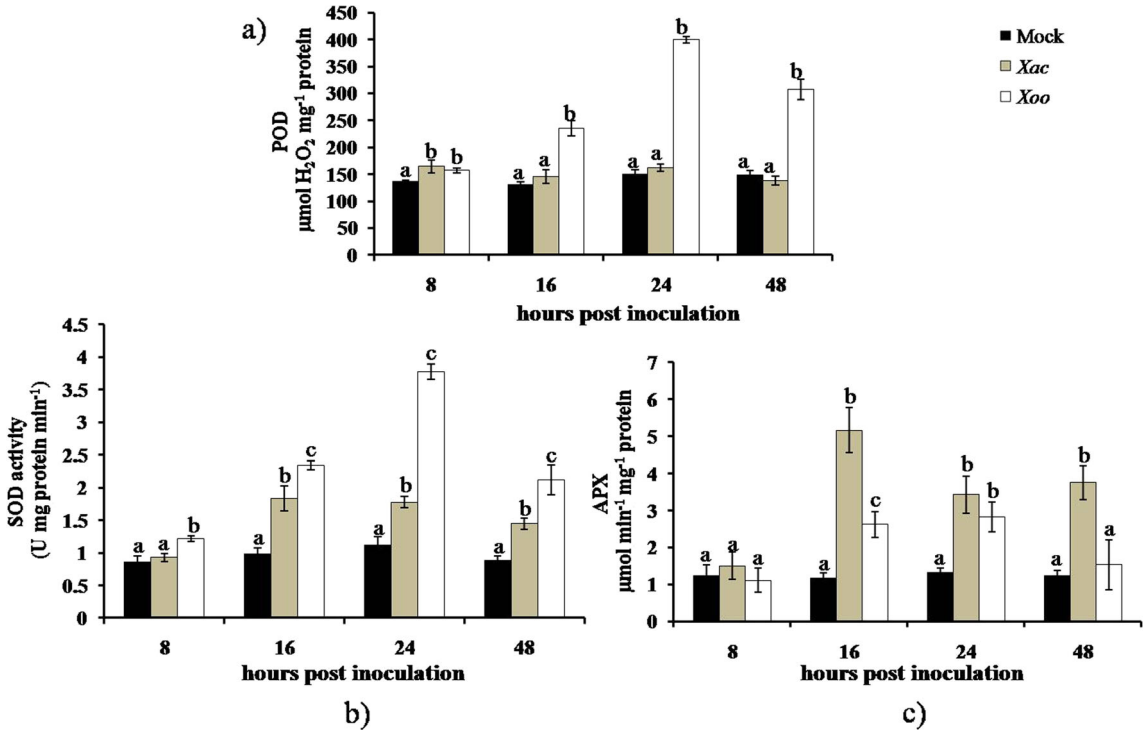

Fig. 6 Activity of ROS metabolizing enzymes during citrus-*Xanthomonas* interaction: **a** Peroxidase (POD), **b** superoxide dismutase (SOD) and **c** ascorbate peroxidase (APX) activities in citrus leaves during interaction with *Xac* and *Xoo* were compared to mock challenge. *Error bars* indicate standard deviation of the mean from three independent experiments. The ANOVA and Tukey test were performed between mock and *Xac*/*Xoo* interaction and between *Xac* vs *Xoo* interaction. *Bars followed by same alphabets* are not significantly different at $P \leq 0.05$

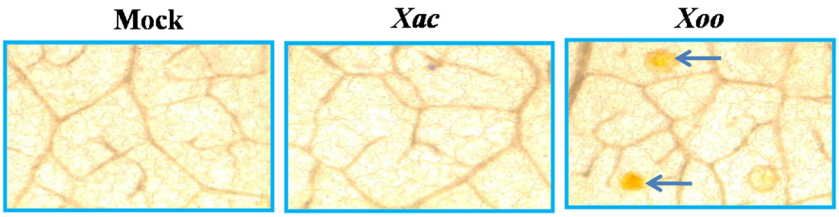

Fig. 7 Lignin deposition during citrus-*Xanthomonas* interaction: Lignin deposition was observed by staining with phloroglucinol at 72 hpi (indicated by *arrows*)

during both host and non-host interactions, while peroxiredoxin got enriched specifically to *Xac* challenge at the early hours (8 hpi). Ascorbic acid metabolism-related proteins like GDP-mannose 3′,5′-epimerase and NAD-dependent epimerase increased only during *Xac* interaction at 48 hpi. Thus, an increase in antioxidant status during compatible interaction favoured survival of host pathogen. The activity of SOD and APX in citrus leaves during compatible and non-host interactions also corroborate with the proteomic information. At 48 hpi, catalase and GST were in low abundance, and Cu/Zn SOD was in high abundance specifically during interaction with *Xoo*, and not in *Xac*-challenged leaves, suggesting accumulation of elevated H_2O_2 levels during non-host interaction (as seen in Figs. 5 and 6). This was evident by increase in SOD activity and H_2O_2 accumulation when measured in the leaf tissue. However, 2.7-fold higher APX activity, low SOD activity and decreased lipid peroxidation during *Xac* interaction indicated high antioxidant status and lower levels of H_2O_2.

Although, an upsurge in ROS triggers signalling pathway(s) to induce the cascade of defence-related gene expression, the response of citrus during non-host interaction was more complex than a simple down-accumulation of potential antioxidant proteins, especially in view of the up-accumulation of monodehydroascorbate reductase and phospholipid hydroperoxide glutathione peroxidase. ROS accumulation, high abundance of a cell death regulator, and Ras-related protein, at 48 hpi during *Xoo* interaction, suggested the role of HR-like cell death in non-host interaction in citrus.

Induction of Defence Responses During Non-Host Interaction

Within the defence/disease category, stress-inducible protein, class I extracellular chitinase, acidic class II chitinase, peroxidase and heat shock proteins (HSP 70, HSP 90 and 17.9 kDa) (Supplementary Table S3, Fig. 4) accumulated during late stages of interaction with non-host pathogen, suggesting an establishment of defence response in the interaction with *Xoo*. Conversely, a decrease in abundance of these proteins occurred at 8 hpi during host (*Xac*) interaction. Gene silencing of HSP90 and HSP70 in *Nicotiana benthamiana* resulted in a severe compromise of HR and NHR along with a concomitant decrease in expression of defence-related genes (Kanzaki et al. 2003) suggesting their involvement in NHR.

Fortification of Citrus Cell Wall During *Xoo* Interaction

Several proteins related to CW synthesis, remodelling, vesicle trafficking and cytoskeleton differentially accumulated during citrus-*Xanthomonas* interaction, where polarized vesicle trafficking has significance in plant–pathogen interactions (Huckelhoven 2007). For instance, vesicle trafficking proteins like clathrin heavy chain and ABC transporter were in low abundance at 8 hpi. While coactomer and dynamin were up-accumulated at 48 hpi, specially during *Xac* challenge (Fig. 6, group I) may be involved in cell division (Huckelhoven 2007). Similarly, CW strengthening proteins like xyloglucan endotransglycosylase/hydrolase (XTH), endo-xyloglucan transferase, ADP-glucose pyrophosphorylase and β-galactosidase were in high abundance only during non-host interaction (Fig. 4, group II).

Proteins involved in the biosynthesis and recycling of methionine, S-adenosylmethionine (SAM), and lignin biosynthesis-related NADP-malic enzyme accumulated at 48 hpi in *Xoo* challenge (Fig. 4, group II). Up-accumulation of methionine/SAM enzymes was known during the HR and required for the acceleration of cell death (Liu et al. 2008). Another protein, O-acetylserine lyase, involved in synthesis of cysteine (a precursor for methionine biosynthesis) also accumulated during *Xoo* challenge indicating a high turnover of methionine during *Xoo* interaction. The increase in methionine/SAM enzymes during *Xoo* interaction may associate with lignin deposition that occurred in *Xoo*-challenged leaves (Fig. 7).

Ethylene biosynthesis proteins like S-adenosyl-L-homocysteinase and ACC oxidase were up-accumulated during *Xac* interaction at 48 hpi, possibly promote CW loosening and elongation during *Xac* interaction. In addition, isoflavone reductase-like protein (one of the key enzymes of isoflavonoid biosynthesis), benzyl alcohol O-benzoyltransferase and cinnamyl alcohol dehydrogenase associated with biosynthesis of monolignols were also in high abundance during non-host interaction. Thymine diphospho (dTDP)-glucose 4-6-dehydratase catalyses synthesis of dTDP-D-glucose, which is a precursor of nucleotide-L-rhamnose (a component of the CW pectin) and secondary metabolites like anthocyanins, flavonoids and triterpenoids was in high abundance during *Xoo* interaction. The accumulation of proteins involved in CW remodelling and secondary metabolism during *Xoo* challenge suggested dynamic change in the composition and secretion

of CW complex to make it more resistant to non-host pathogen (also can be seen in Fig. 7), whereas, increase in the pectin esterase protein species (at 48 hpi) during *Xac* interaction may be involved in CW loosening and cell expansion during canker formation.

Repression of Photosynthesis and Carbon Metabolism During Citrus-*Xanthomonas* Interaction

Rubisco and rubisco activase were in low abundance during both *Xac* and *Xoo* interactions at 48 hpi (Fig. 4, group III). Glycolysis and Krebs cycle enzymes up-accumulated early (8 hpi) during *Xac* interaction but down-accumulated during *Xoo* challenge. At 48 hpi, they were down-accumulated in host and non-host interactions (Fig. 4). In addition, biochemical analysis indicated the decrease in oxygen evolution at 48 hpi during both *Xac* and *Xoo* challenge indicated a possible decrease of photosynthetic rate (Supplementary Fig. S3) and in agreement with earlier findings (Bonfig et al. 2006; Garavaglia et al. 2010). Low abundance of photosynthesis-related proteins was also known in incompatible host-pathogen interactions (Matsumura et al. 2003). Tao et al. (2003) reported a decrease in photosynthesis in *Arabidopsis* with the avirulent strain than with the virulent strain of *Pseudomonas syringae*, while qualitatively, the responses in both interactions are similar. Photosynthetic function in the host plant compromised under biotic stress and resulted in reallocation of energy to express defence response. In the present gel-based proteome analysis, two chlorophyll a/b-binding protein species involved in providing balance excitation energy between photosystems I and II (Kundu et al. 2011) accumulated in both compatible and non-host citrus-*Xanthomonas* interactions.

Modulation of protein synthesis/folding and degradation

Next to energy-related proteins, proteins involved in translation were in low abundance at late hours (48 hpi) of interaction with *Xoo* (Fig. 3). Elongation factor Tu and 40S and 60S ribosomal protein species were in low abundance during both *Xac* and *Xoo* challenge at 48 hpi. A few other ribosomal protein homologues of chloroplast ribosomal proteins (Supplementary Table S3) were also in low abundance during non-host interaction, suggesting turning off of protein synthesis.

In the present study, protein disulfide isomerase, ubiquitin conjugation enzyme, peptidyl-prolyl *cis-trans* isomerase and chaperone protein ClpB1 accumulated differentially during *Xoo* interaction (Fig. 4), whereas, TCP-1/cpn60 chaperonine and 20S proteasome were differentially accumulated during both the interactions. Emerging evidence on the ubiquitin-proteasome pathway in implementation of the plant defence response (Austin et al. 2002; Liu et al. 2002) indicates the essentiality of modulation of protein synthesis/folding and degradation-related proteins in plant–non-host pathogen interactions.

Conclusion

Two alternative and yet complementary proteomic approaches were used to analyse the response of citrus during compatible (*Xac*) and non-host (*Xoo*) interactions. The present study revealed that molecular response of citrus towards non-host pathogen (*Xoo*) was mainly associated with consistent accumulation of proteins associated with ROS metabolism, signalling, cell wall reinforcement and lignin deposition, supported in part by biochemical analyses. Our results suggest the significance of such proteins in the production of relevant products to mount defensive barrier against non-host pathogens.

Acknowledgments We thank UGC-CAS programme and Proteomics Facility (DBT-CREBB) of School of Life Sciences and DST-FIST facility of Plant Sciences Department at University of Hyderabad. TSR acknowledges the research fellowship from DBT-CREBB and DST-INSPIRE, India. The research performed in Iwate University was in part supported by Grants-in-Aid (#22120003 and #24370018to MU and #24-7373 to DT) from Japan Society for the Promotion of Science (JSPS).

Conflict of interests The authors declare that they have no competing interests.

Author's contributions TSR carried 2DE, biochemical analysis and statistical analysis. TSR and DT performed nano-LC-MS/MS. ARP designed the experiments, and TSR, DT, MU and ARP wrote the final draft of the manuscript. All authors read and approved the manuscript.

References

An C, Mou Z (2012) Non-host defense response in a novel *Arabidopsis-Xanthomonas citri* subsp. *citri* Pathosystem. PLoS One 7:e31130

Asirvatham VS, Watson BS, Sumner LW (2002) Analytical and biological variances associated with proteomic studies of *Medicago truncatula* by two-dimensional polyacrylamide gel electrophoresis. Proteomics 2:960–968

Austin MJ, Muskett P, Kahn K et al (2002) Regulatory role of SGT1 in early R gene-mediated plant defenses. Science 295:2077–2080

Beauchamp C, Fridovich I (1971) Superoxide dismutase: improved assays and an assay applicable to acrylamide gels. Anal Biochem 44: 276–287

Bevan M, Bancroft I, Bent E et al (1998) Analysis of 1.9 Mb of contiguous sequence from chromosome 4 of *Arabidopsis thaliana*. Nature 391:485–488

Bonfig KB, Schreiber U, Gabler A et al (2006) Infection with virulent and avirulent *P. syringae* strains differentially affects photosynthesis and sink metabolism in *Arabidopsis* leaves. Planta 225:1–12

Caraux G, Pinloche S (2005) PermutMatrix: a graphical environment to arrange gene expression profiles in optimal linear order. Bioinformatics 21:1280–1281

Daurelio LD, Petrocelli S, Blanco F et al (2011) Transcriptome analysis reveals novel genes involved in nonhost response to bacterial infection in tobacco. J Plant Physiol 168:382–391

Daurelio LD, Romero MS, Petrocelli S et al (2013) Characterization of *Citrus sinensis* transcription factors closely associated with the nonhost response to *Xanthomonas campestris* pv. *vesicatoria*. J Plant Physiol 170:934–942

Garavaglia BS, Thomas L, Zimaro T et al (2010) A plant natriuretic peptide-like molecule of the pathogen *Xanthomonas axonopodis* pv. *citri* causes rapid changes in the proteome of its citrus host. BMC Plant Biol 10:e8950

Heath RL, Packer L (1968) Photoperoxidation in isolated chloroplast. I. Kinetics and stoichiometry of fatty acid peroxidation. Arch Biochem Biophys 125:189–198

Henkel AW, Bieger SC (1994) Quantification of proteins dissolved in an electrophoresis sample buffer. Anal Biochem 223:329–331

Huckelhoven R (2007) Cell wall-associated mechanisms of disease resistance and susceptibility. Annu Rev Phytopathol 45:101–127

Isaacson T, Damasceno CM, Saravanan RS et al (2006) Sample extraction techniques for enhanced proteomic analysis of plant tissues. Nat Protoc 1:769–774

Kang L, Li J, Zhao T et al (2003) Interplay of the *Arabidopsis* nonhost resistance gene NHO1 with bacterial virulence. Proc Natl Acad Sci U S A 100:3519–3524

Kanzaki H, Saitoh H, Ito A et al (2003) Cytosolic HSP90 and HSP70 are essential components of INF1-mediated hypersensitive response and non-host resistance to *Pseudomonas cichorii* in *Nicotiana benthamiana*. Mol Plant Pathol 4:383–391

Kundu S, Chakraborty D, Pal A (2011) Proteomic analysis of salicylic acid induced resistance to Mungbean Yellow Mosaic India Virus in *Vigna mungo*. J Proteomics 74:337–349

Li B, Takahashi D, Kawamura Y et al (2012a) Comparison of plasma membrane proteomic changes of *Arabidopsis* suspension-cultured cells (T87 Line) after cold and ABA treatment in association with freezing tolerance development. Plant Cell Physiol 53:543–554

Li W, Xu Y-P, Zhang Z-X et al (2012b) Identification of genes required for nonhost resistance to *Xanthomonas oryzae* pv. *oryzae* reveals novel signaling components. PLoS One 7:e42796

Liu H, Wang Y, Xu J et al (2008) Ethylene signaling is required for the acceleration of cell death induced by the activation of *AtMEK5* in *Arabidopsis*. Cell Res 18:422–432

Liu Y, Schiff M, Serino G et al (2002) Role of SCF ubiquitin-ligase and the COP9 signalosome in the N genemediated resistance response to tobacco mosaic virus. Plant Cell 14:1483–1496

Ma QU (2007) Small GTP-binding proteins and their functions in plants. J Plant Growth Regulation 26:369–388

Matsumura H, Reich S, Ito A et al (2003) Gene expression analysis of plant host-pathogen interactions by SuperSAGE. Proc Natl Acad Sci U S A 100:15718–15723

Meunier B, Dumas E, Piec I et al (2007) Assessment of hierarchical clustering methodologies for proteomic data mining. J Proteome Res 6:358–366

Nakano A, Asada K (1987) Purification of ascorbate peroxidase in spinach chloroplasts: its inactivation in ascorbate-depleted medium and reactivation by monodehydroascorbate radical. Plant Cell Physiol 28:131–140

Nouri M-Z, Komatsu S (2010) Comparative analysis of soybean plasma membrane proteins under osmotic stress using gel-based and LC MS/MS-based proteomics approaches. Proteomics 10:1930–1945

Nurnberger T, Lipka V (2005) Non-host resistance in plants: new insights into an old phenomenon. Mol Plant Pathol 6:335–345

Nurnberger T, Scheel D (2001) Signal transmission in the plant immune response. Trends Plant Sci 6:372–379

Oh S-K, Lee S, Chung E et al (2006) Insight into types I and II nonhost resistance using expression patterns of defense-related genes in tobacco. Planta 223:1101–1107

Overmyer K, Brosche M, Kangasjarvi J (2003) Reactive oxygen species and hormonal control of cell death. Trends Plant Sci 8:335–342

Rani TS, Podile AR (2014) Extracellular matrix-associated proteome changes during non-host resistance in citrus-*Xanthomonas* interactions. Physiol Plant 150:565–579

Roberts MR, Salinas J, Collinge DB (2002) 14-3-3 proteins and the response to abiotic and biotic stress. Plant Mol Biol 50:1031–1039

Schulze-Lefert P, Panstruga R (2011) A molecular evolutionary concept connecting nonhost resistance, pathogen host range, and pathogen speciation. Trends Plant Sci 16:117–125

Senthil-Kumar M, Mysore KS (2013) Nonhost resistance against bacterial pathogens: retrospectives and prospects. Annu Rev Phytopathol 51:19.1–19.21

Shevchenko A, Wilm M, Vorm O et al (1996) Mass spectrometric sequencing of proteins silver-stained polyacrylamide gels. Anal Chem 68:850–858

Takahashi D, Kawamura Y, Uemura M (2013) Changes of detergent-resistant plasma membrane proteins in oat and rye during cold acclimation: association with differential freezing tolerance. J Proteome Res doi.org/10.1021/pr400750g

Takahashi D, Kawamura Y, Yamashita T et al (2012) Detergent-resistant plasma membrane proteome in oat and rye: similarities and dissimilarities between two monocotyledonous plants. J Proteome Res 11: 1654–1665

Talla S, Riazunnisa K, Padmavathi L et al (2011) Ascorbic acid is a key participant during the interactions between chloroplasts and mitochondria to optimize photosynthesis and protect against photoinhibition. J Biosci 36:163–173

Tao Y, Xie Z, Chen W et al (2003) Quantitative nature of *Arabidopsis* responses during compatible and incompatible interactions with the bacterial pathogen *Pseudomonas syringae*. Plant Cell 15:317–330

Thordal-Christensen H, Zhang Z, Wei Y et al (1997) Subcellular localization of H_2O_2 in plants. H_2O_2 accumulation in papillae and hypersensitive response during the barley-powdery mildew interaction. Plant J 11:1187–1194

Uma B, Rani TS, Podile AR (2011) Warriors at the gate that never sleep: non-host resistance in plants. J Plant Physiol 168:2141–2152

Vallet C, Chabbert B, Czaninski Y et al (1996) Histochemistry of lignin deposition during sclerenchyma differentiation in alfalfa stems. Annu Bot 78:625–632

Velikova V, Yordanov I, Edreva A (2000) Oxidative stress and some antioxidant systems in acid rain-treated bean plants: protective roles of exogenous polyamines. Plant Sci 151:59–66

Wang X, Li X, Li Y (2007) A modified commassie brilliant blue staining method at nanogram sensitivity compatible with proteomic analysis. Biotechnol Lett 29:1599–1603

Zamany A, Liu J-J, Ekramoddoullah AKM (2012) Comparative proteomic profiles of *Pinus monticola* needles during early compatible and incompatible interactions with *Cronartium ribicola*. Planta 236: 1725–1746

Zimaro T, Gottig N, Garavaglia BS et al (2011) Unraveling plant responses to bacterial pathogens through proteomics. J Biomed Biotechnol 2011:354801